QUANTITATIVE ANALYSIS OF MINERALS ACROSS THE ORIENTALE BASIN ON THE MOON. Jinzhu Ji[1,2,3], Jianzhong Liu[1], James W. Head[2], Carle M. Pieters[2], Honglei Lin[3,4]. [1]Center for Lunar and Planetary Science, Institute of Geochemistry, Chinese Academy of Sciences, Guiyang 550081, China, email: jijinzhu@mail.gyig.ac.cn, [2]Department of Earth, Environmental and Planetary Sciences, Brown University, Providence, RI 02912 USA, [3]University of Chinese Academy of Sciences, Beijing 100049, China, [4]Institute of Remote Sensing and Digital Earth, Chinese Academy of Sciences, Beijing 100101, China.

Introduction: The Orientale basin is one of the youngest impact multi-ringed basins on the Moon [e.g. 1-4]. Unlike some lunar basins it has not been significantly filled with mare basalt subsequent to its formation, and thus provides access to materials exposed in the basin interior and floor, including the melt sheet. Mineralogy and petrology is one of the most important clues for the formation of mutil-rings, impact melt sheet, mascon and even the history of the thermal evolution of the Moon [5]. Therefore, the quantitative analysis of minerals is very critical. Remotely acquired reflectance spectra, combined with spectroscopic, chemical, and mineralogical data acquired in the Reflectance Experiment Laboratory (RELAB) from returned lunar samples, can provide constraints on understanding and establishing compositional information about these unsampled surfaces of the Moon.

Data: The Moon Mineralogy Mapper (M^3) acquired high spatial and spectral resolution data of the Orientale basin with 140 m/pixel in 85 spectral bands from 0.43 to 3.0 mm. These data are from the first optical period (OP1b), including thermal corrections and photometric corrections derived from local topography [e.g. 6-10]. In this study, the data were truncated into 3~72 bands from 0.54 to 2.46 mm.

Endmembers were selected from the RELAB data of lunar returned samples to build the spectral library (http://www.planetary.brown.edu/relab/) (Fig. 1 and Table 1), including 16 mineral separates and 5 lunar soil with particle size < 45 μm; all spectra were obtained at i=30 degrees, e=0 degrees [11- 13].

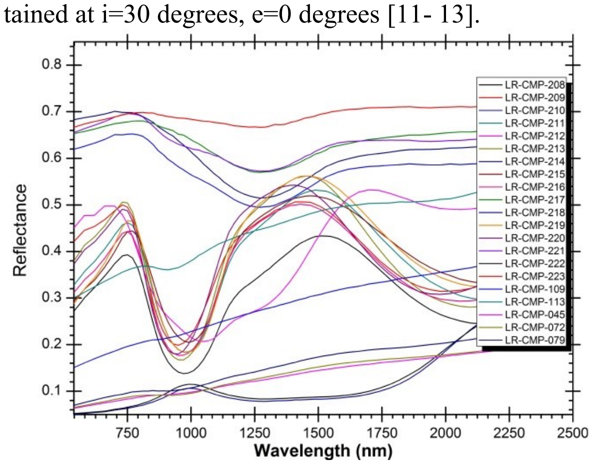

Figure 1. *Endmembers in spectral library*

Table 1. *The laboratory measured endmembers used in this study*

SimpleID	SampleName
LR-CMP-208	15058,276 brown pyroxene D <45 um
LR-CMP-209	15058,276 green pyroxene D <45 um
LR-CMP-210	15058,276 plagioclase D <45 um
LR-CMP-211	15555,965 reddish-brown pyroxene D <45 um
LR-CMP-212	15555,965 olivine D <45 um
LR-CMP-213	15555,965 light-brown pyroxene D <45 um
LR-CMP-214	15555,965 plagioclase D <45 um
LR-CMP-215	70017,535 deep-brown pyroxene D <45 um
LR-CMP-216	70017,535 light-brown pyroxene D <45 um
LR-CMP-217	70017,535 plagioclase D <45 um
LR-CMP-218	70017,535 ilmenite D <45 um
LR-CMP-219	70035,188 dark-brown pyroxene D <45 um
LR-CMP-220	70035,188 light-brown pyroxene D <45 um
LR-CMP-221	70035,188 plagioclase D <45 um
LR-CMP-222	70035,188 ilmenite D <45 um
LR-CMP-223	62241,21 plagioclase D <45 um
LR-CMP-045	70181,147 mare soil
LR-CMP-072	12001,873 mare soil
LR-CMP-079	15071,167 mare soil
LR-CMP-109	61141,75 highland soil
LR-CMP-113	67461,142 highland soil

Methods: The quantitative analysis method combines Hapke modeling with a sparse unmixing algorithm [14]. The Hapke model provides the relation between reflectance and single-scattering albedo by considering the nonlinear mixed effects of minerals [15, 16]. The single-scattering albedo of an intimate mineral mixture mixes linearly. Thus, linear unmixing techniques can be used to estimate the abundances of minerals. The sparse unmixing algorithm can decompose pixels using a relatively large spectral library. Finally, minerals can be retrieved without assuming compositions and spectra from original data. The main steps of this method are: 1) building endmember library, 2) calculating the single-scattering albedo (SSA) data and endmembers using Hapke radiative transfer modeling, respectively, 3) sparse unmixing the result of SSA data.

Results: We used the method above to produce mineral abundance maps of Orientale basin (Fig. 2). In this region, the main materials are highland and mare soils that contain abundant agglutinates produced by space weathering. We can also identify the presence of different minerals, which have a strong spectral absorption that can represent the host mineral of this region. For instance, in the Maunder Crater region(Fig. 3a), the measured and modeled single-scattering albedo spectra fit very well with the value of root-mean square error lower than 0.01 (Fig. 3b) and we also can acquire the type and abundance of minerals in this region (Fig. 3c). For example: at point 1 at the north rim of Maunder Crater, there is 34% of highland soil, 65 % of plagioclase and lower than 1% of augite and ilmenite. Thus this region is hosted by plagioclase and we can infer that the subsurface lithology of this region is anorthositic; at point 7 on the eject deposit of Maunder Crater, there is 55% of mare soil, 1% of plagioclase, 6% of augite, 13% of olivine and 25% of ilmenite, and we can infer that Maunder penetrated down through anorthosite layers into lower-crust, providing estimated boundary depth and lithological stratigraphy [9].

Conclusion: We use the quantitative analysis method that combines the Hapke model with a sparse unmixing algorithm to retrieve the minerals and their abundance at Orientale basin region, which can provide important clues to assess the formation of basin-rings, the impact melt, mascon and even the history of the thermal evolution of the Moon. Further work is being conducted to select fresh region of impact melt.

Acknowledgements: This work was supported by the National Natural Science Foundation of China (Grant No. 41490634 and No. 41773065) and National Science and Technology Infrastructure Work Projects (Grant No. 2015FY210500).

References: [1] Wilhelms D. (1987) *USGS* PP-1348. [2] Head J. W. (1974) *The Moon*, 11, 327–356. [3] Head J. W. (1993) *JGR*, 98, 17,149–17,181. [4] Spudis P. (1993) *Geology of Multi-Ring Impact Basins*, Cambridge. [5] Head J. W. et al. (2012) *AGU Fall Meeting Abstracts*. [6] Pieters C. M. et al. (2009) *LPSC XL,* Abstract #2052. [7] Pieters C. M. et al. (2009) *Curr. Sci.*, *96*, 500–505. [8] Green R. et al. (2011) *LPSC XLII*. [9] Besse et al., (2013) *Icarus, 222*, 229–242. [10] Li S. and Ralph E. M. (2016) *JGR Planets 121*, 2081-210. [11] Pieters C. M. et al. (2000) *LPSC XXXI*, Abstract #1865. [12] Taylor L. A. et al. (2001) *JGR*, *106*, 27,985–28,000. [13] Isaacson et al., (2011) *Meteor. Planet. Sci.*, *46*, 228–251. [14] Lin H. and Zhang X. (2017) *Icarus*, *288*, 160–171. [15] Hapke B. (1981) *JGR, 86*, 3039–3054. [16] Heylen R. et al. (2014) *IEEE J. Sel. Topics Appl. Earth Obs. Remote Sens*., *7*, 1844–1868.

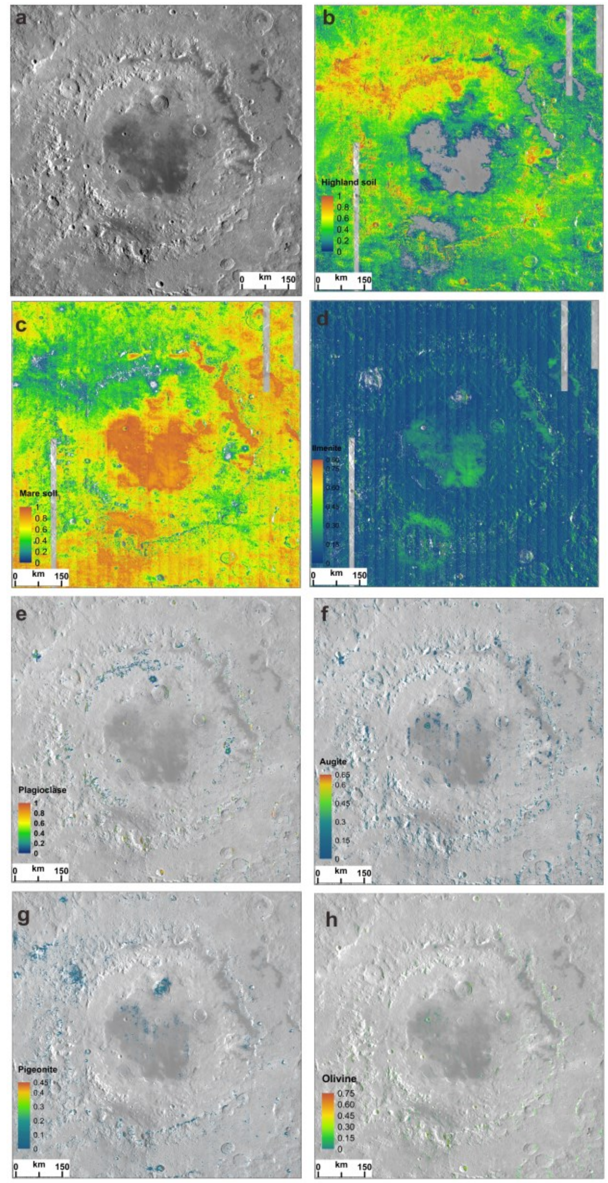

Figure 2. Orientale basin region (a, WAC image) and the abundance maps of b) highland soil, c) mare soil, d) ilmenite, e) plagioclase, f) augite, g) pigeonite, g) olivine.

Figure 3. Maunder crater region (a): example measured and modeled single-scattering albedo spectra (b) and abundance of each minerals or soil (c). All the ROI points are averaged by 4 ×4 pixels.